A numerical study of the mesoscale variability in the Adriatic Sea

P. Oddo [(1)] *, N. Pinardi*[(2)]

[(1)] *Istituto Nazionale di Geofisica e Vulcanologia,*

Bologna, Italy

[(2)] *Centro Interdipartimentale per la Ricerca in Scienze Ambientali, Università di Bologna*

Ravenna, Italy

Date of Submission ***August 30, 2007***

Corresponding author address*: Paolo Oddo, Istituto Nazionale di Geofisica e Vulcanologia,*

Via Aldo Moro 44, 40127 Bologna Italy.

Tel.: ++39 0514151483. Fax: ++39 051 4151499.

E-mail: oddo@bo.ingv.it

Abstract

The Adriatic Sea mesoscale and its inter-annual variability is investigated by means of a high-resolution numerical ocean model with approximately 2 km resolution. The ocean model used is based on the Princeton Ocean Model (POM, Blumberg and Mellor 1987) which has been modified in the advection scheme and the vertical velocity surface boundary condition. The simulation spans 6 years starting from January 1999 till December 2004. The surface forcing is interactively computed using European Centre for Medium Range Weather Forecast (ECMWF) operational atmospheric fields and climatological precipitation, while river runoff is obtained combining daily Po river (the main Adriatic river) data together with climatological estimates for all the other rivers. The model results have been validated by an extended comparison with in situ and remote sensing observations.

The simulated variability exhibits evident similarities with the actual mesoscale variability, in terms of location, nature and temporal evolution of the features. The major results concern the spatial and temporal variability of Eddy and Mean Kinetic Energy (EKE and MKE) and the baroclinic energy conversion term contained in the buoyancy work time rate. We show for the first time evidence of baroclinic instability at the level of major sub-basin scale structures such as the Western Adriatic Coastal Current. Furthermore, the seasonal and inter-annual variability of mean and eddy kinetic energy is correlated with surface forcing (wind stress work) and Po runoff.

Introduction

The Adriatic Sea is a marginal basin of the Mediterranean Sea extending between the Italian and the Balkan Peninsulas (Fig.1). It extends from 40° to 45° 45' N going from the Gulf of Trieste to the Strait of Otranto, the latter linking the Adriatic to the Ionian Sea. The general circulation characteristics and their seasonal and inter-annual variations have been largely investigated in the past years through both direct observations (Artegiani et al 1997a and 1997b, Poulain 2001) and numerical simulations (Zavatarelli *et al* 2002, Zavatarelli and Pinardi 2003, Oddo *et al* 2005). However, the mesoscale variability has only been marginally investigated because very high-resolution models, or large number of observations, are required. The first observational and modelling study of mesoscale variability was done at the beginning of the nineties and only for the middle Adriatic Sea (Paschini et al, 1993, Masina and Pinardi, 1994). Only recently observational (Poulain 2001, Ursella *et al* 2007) and numerical (Cushman-Roisin *et al* 2007) studies have partially investigated the nature of the Adriatic mesoscales for the whole basin.

In this paper, the Adriatic mesoscale dynamics is investigated through a very high-resolution numerical model with realistic inter-annual atmospheric forcing. The interest in Adriatic mesoscale dynamics derives from the fact that fronts, jets, meanders and eddies are ubiquitous across the Adriatic Sea, and it is believed that they play a fundamental role in the ocean response to buoyancy forcing, winds and topographic gradients. Our understanding of this variability, however, is relatively basic at the current time, since most of the models up to now could not effort enough horizontal and vertical resolution and only few datasets have adequate temporal and spatial resolution for the mesoscales to emerge in the whole basin.

Using surface drifter derived circulation, spatial and temporal variability of eddy and mean surface kinetic energy has been recently studied (Poulain 2001, Ursella *et al* 2007). Both the

components of the kinetic energy have been found to reach maxima values close to the coasts (especially along the Italian coast in the Western Adriatic Current, WAC, region), while minima occur in the open sea regions. Only north of the Jabuka Pit (Fig.1), where large bathymetric gradient occurs, high kinetic energy values are detected also in the open sea region. Eddy and Mean components of the kinetic energy are characterized by a well marked seasonal cycle (with some inter-annual variability, Ursella *et al* 2007), with minimum values occurring during spring-summer seasons and maxima in autumn-winter.

In a recent numerical study (Cushman-Roisin *et at* 2007), baroclinic instability has been identified as the major responsible of mesoscale variability in the coastal area, while potential-vorticity stretching associated with steep bottom topography as the main mechanism for the mesoscale occurrence in the central part of the basin.

In particular, the role of mesoscale dynamics in a relatively shallow basin, driven by both river runoff and intense exchanges with the atmosphere, is a relatively new problem in coastal oceanography. The development of mesoscale dynamics at shallow depths, where external forcings have the same importance of internal dynamical processes is interesting per se. In addition this study is important for the understanding of the Adriatic Sea circulation for practical purposes. In fact, recently the Adriatic Sea has been the site of development of operational oceanographic models (Oddo *et al.*, 2006) and forecasting requires the knowledge of the processes underlying the circulation variability.

This paper tries to give for the first time an overall assessment of the mesoscale variability in connection with atmospheric forcing and energy redistribution processes. The study concentrates on the energy content of the circulation, subdividing its mean and eddy contributions in different sub-regions.

The mesoscale is characterized by the first baroclinic Rossby radius of deformation that in the middle and northern Adriatic Sea is about 3-5 km (Paschini *et al*., 1993, Masina and Pinardi, 1994; Bergamasco *et al*., 1996). The eddies can have a diameter of 20 km, during the high stratification season (Paschini *et al.,* 1993) but in the Northern Adriatic Sea the eddy diameter could be smaller, as well as the local and seasonal Rossby radius of deformation. The Adriatic Sea in fact is completely mixed during winter and thus the first baroclinic Rossby radius of deformation almost vanishes in this season.

In order to start the study of mesoscales variability we follow a classical approach where the flow field is subdivided into mean and eddy components and kinetic energy budgets are studied in different sub-regions as done many times in the Atlantic (e.g. Harrison and Robinson, 1978 or Jochum *et al*. 2004). In this context, the baroclinic conversion term is studied in order to detect baroclinic and/or barotropic instabilities of the normal type (Pedlosky, 1987). This analysis allows, for the first time, to draw some conclusions on the source of energy for the mesoscales in this basin.

In Section 2 a description of the model and numerical experiments is given, Section 3 offers the kinetic analysis of the simulation results, in Section 4 the conclusions are given.

2. Model design and Experiment description

The model used in this work is based on the Princeton Ocean Model (POM, Blumberg and Mellor, 1987). The model has been implemented with a regular horizontal grid having approximately 2.2 km resolution (1/22° of latitude and longitude) and 31 sigma layers in the vertical. The model boundary is south of the Otranto Strait along the 39° parallel. The minimum depth is 10 m but the Adriatic has a realistic coastline and between 0 and 10 meter depth the slope has been flattened.

The surface fluxes are interactively computed using model predicted sea surface temperature and realistic atmospheric data. The model uses the same bulk formulae to compute surface fluxes described in Oddo *et al.* (2005). The atmospheric data (air temperature, relative humidity, cloud cover and both wind components) are analyses with 0.5° horizontal resolution and 6hrs frequency, provided by the European Centre for Medium Range Weather Forecast (ECMWF).

In order to allow the model to reproduce adequately the Adriatic mesoscale dynamics some numerical parameterizations have been improved.

Real freshwater input has been used in the surface boundary condition for the vertical velocity that becomes:

$$w\big|_{z=h} - \left(\frac{\partial h}{\partial t} + \bar{v} \cdot \nabla h \right)\Bigg|_{z=h} = (E - P - R) \qquad (1)$$

where w is the vertical velocity, h is the surface elevation, E is the evaporation, P is the precipitation and R indicates the rivers runoff. The two critical components of the water flux are the precipitation and the runoff. For precipitation we use the climatological monthly mean values from Legates and Wilmott (1990) since ECMWF estimates in this small region are believed to be large. For river runoff, daily values are used for the Po while only climatological values are considered for the other forty-eight (rivers and springs) sources (Raicich, 1994). Following the hypothesis made in Oddo *et al* (2005), concerning a possible overestimation of these climatological values in the past ten years, we reduced the prescribed data for the Croatian part by a factor 0.3 (this factor derives from sensitivity studies).

The Po runoff is specified daily taking the values at the closing point of the drainage basin (PonteLagoScuro) and partitioned over several grid points approximately representing the proportion of the fresh water discharge through the mouth of the delta (Provini *et al.* 1992).

A further difference with the previous POM simulations in the Adriatic Sea (Oddo *et al*. 2005, Oddo *et al.* 2006, Zavatarelli *et al*. 2002, Zavatarelli and Pinardi 2003) regards the advection scheme. A flux limiting advection scheme (MUSCL, Estubier and Lévy, 2000) has been implemented allowing a better reproduction of the horizontal and vertical gradients.

For initial and lateral boundary conditions (temperature, salinity and velocity fields) data are taken from a 1/16° horizontal resolution model of the entire Mediterranean Sea (Tonani *et al*., 2007). The lateral boundary data are provided daily. The definition of the nested open boundary conditions is based on Oddo *et al* (2005).

The simulation spans the period from January 1999 to December 2004, results for year 1999 are not shown as this year is considered to represent the model spin up. The model validation through comparison with in situ data is given in the Appendix-B.

3. Model Results

The mean winter and summer (winter is from January to April and summer from July to October, according to Artegiani et al. 1997a, b) surface velocity fields are shown in Fig.2. It is evident that the model reproduces well the known Adriatic circulation and its seasonal variability (Poulain, 2001).

The large-scale circulation pattern appears substantially similar to previous simulations considering other years (Oddo *et al.* 2005, Pullen *et al.* 2003, Pullen *et al.* 2006, Zavatarelli *et al.* 2002, Mantziafou and Lascaratos 2004); major structures such the WAC along the Italian coast; the EAC along the Croatian coast, the Southern, Middle and Northern Adriatic Gyres are reproduced with their own seasonal variability. However, the higher horizontal and vertical resolution of this model together with the reduced viscosity-diffusivity, seem to allow

for a better simulation of the amplitude and structure of the Western Adriatic Current (Artegiani *et al.*, 1997).

In order to do the energy analysis, the velocity field is decomposed into mean component and eddy part, i.e.

$$(u,v) = (U + u', V + v') \tag{2}$$

where the U and V indicate the mean while the primes the eddy components respectively. The mean fields, in this study, are defined as the monthly averages over the period 2000-2004.

We then define the Mean Kinetic Energy (MKE) and Eddy Kinetic Energy (EKE) as:

$$\begin{aligned} \mathbf{MKE} &= \frac{1}{2}(U^2 + V^2) \\ \mathbf{EKE} &= \frac{1}{2}(u'^2 + v'^2). \end{aligned} \tag{3}$$

The monthly average Total Kinetic Energy (TKE) is then equal to MKE plus EKE. If the average is done in another time interval then the TKE is defined simply as the square of (2)..

The equation for the time evolution of EKE can be derived from momentum equation applying the above decomposition (2), and after proper manipulations it derives:

$$\begin{aligned} &\frac{\partial EKE}{\partial t} + \vec{U} \cdot \vec{\nabla} EKE + \vec{u}' \cdot \vec{\nabla} EKE = \\ &\quad - \vec{u}' \cdot \vec{\nabla} p' - g w' \rho' + \rho_0 \left[- \vec{u}' \cdot \left(\vec{u}' \cdot \vec{\nabla} \vec{U} \right) + \vec{u}' \cdot \underline{\left(\vec{u}' \cdot \vec{\nabla} \vec{u}' \right)} + \vec{\nabla} \cdot \left(A_k \vec{\nabla} EKE \right) \right] \end{aligned} \tag{4}$$

where g is the gravitational acceleration and ρ' arises from the decomposition of the instantaneous density field into a no-motion part $\overline{\rho}(z)$, a time independent component $\overline{\overline{\rho}}(x, y, z)$ and a spatial and temporal varying component $\rho'(x, y, z, t)$:

$$\rho = \overline{\rho}(z) + \overline{\overline{\rho}}(x, y, z) + \rho'(x, y, z, t)\,. \tag{5}$$

In (4) w' is the vertical velocity obtained applying (2) to the total vertical velocity field. The derivation of (4) is given in Appendix-A together with the explanations of the physical meaning of all the terms (see also Orlanski and Katzfey 1991).

In this study we also try to focus on the energy transfer between Eddy Available Potential Energy (EAPE) and EKE (Lorenz 1955, Pedlosky 1987) by studying the spatial distribution and time variability of the Baroclinic Eddy Conversion (BEC) term, the second term on the right hand side of (4). BEC is the well known buoyancy work term that appears with opposite sign in the EAPE and EKE time evolution equations and thus defines the conversion between the two forms of energies. Positive values of BEC indicate an energy transfer from EAPE to EKE (in literature this process has been related to the Eady instability process, Pinardi and Robinson, 1986), negative values indicate that the eddy field motion restore vertical and/or horizontal shears with a net growth of EAPE (also called inverse baroclinic conversion). We will use the BEC term to show the presence of baroclinic instability at the seasonal time frequency in different sub-portions of the basin.

3.1 Kinetic Energy Budgets

In Fig.3 the climatological time series of TKE (here considered as the sum of MKE and EKE) integrated over the upper 5 m and averaged over the whole Adriatic basin is shown together with the corresponding values obtained from the 1990-1999 lagrangian observations of Poulain (2001). The time series are only in partial agreement; the most relevant difference is the absence in the simulated time series of the two (spring and summer) relative maxima. The differences in values and shape of the two curves might be due to the different time periods considered by the model simulation and the observations (observations were collected in the

1990-1999 period). In addition, drifters space sampling in very inhomogeneous and the EKE from observations could be more representative of smaller areas than the overall basin. On the model side, the atmospheric forcing is still being at relatively low resolution and the river runoff is parameterized in a simple way. However, in both time series the minimum energy levels are observed between February and July with values ranging between 100 and 130 cm^2 s^{-2}. In the observations, there is a sharp increase of energy starting in August marking the beginning of a 6-month high energy period (August to January, with values exceeding 150 cm^2 s^{-2}). The model fails to have this rapid growth even if for the same period it reaches the largest kinetic energy values.

Moreover other studies (Ursella *et al* 2007), performed using drifters in the Northern and Middle Adriatic for the period between September 2002 and December 2003, depicted lower values of surface MKE and EKE with relatively large inter-annual variability and the absence of the spring maximum. This reinforces our hypothesis that the sampling period is crucial due to the intrinsic temporal variability of the system.

The climatological seasonal cycle of the near-surface kinetic energy averaged over the whole Adriatic Sea is well correlated with the wind stress work ($\bar{u} \cdot \bar{\tau}$, where $\bar{u}$ is the surface current and $\bar{\tau}$ the wind stress vector, Pedlosky 1987) shown in Fig.4, which reaches the maximum values in winter and the minimum in summer. The August-September high energy value in the observations (Fig.3) is not reflected directly in the wind forcing: this on one hand strengthens our hypothesis of the relevance of the sampling period, on the other hand suggests the possibility that the high kinetic energy peak is due to internal energy re-distribution processes (energy converted from EAPE to EKE). However, the model does not seem to reproduce well this peak and we can only speculate about its nature. The Po runoff peaks

(Fig.4) do not seem to have relevant correlations with the kinetic energy maxima except for the autumn peak for both the observations and model results.

Based on the simulated energy distribution and observed oceanographic characteristics of the Adriatic Sea (Artegiani *et al*., 1997a and b), 4 regions have been defined and separately analyzed: the WAC region, between the Po delta and Otranto Strait along the Italian coast; the Northern region, delimited by 100 m bathymetry north of the Jabuka Pit; the Middle region, with the southern boundary across the basin starting from the Gargano Peninsula; and the Southern Adriatic region. The limits of these sub-regions are depicted in Fig.1. It has to be stressed that the WAC is defined here as the entire current flowing south-eastward along the Italian Peninsula including also the western limbs of the cyclonic gyres. This definition is similar to the one adopted by Poulain (2001) but differs from the one used in Artegiani *et al*. (1999) and Hopkins *et al*. (1999).

The MKE, EKE and BEC have been spatially averaged over these regions as follows:

$$\vartheta(t) = \frac{1}{V}\int_{h1}^{h2}\int_{y1}^{y2}\int_{x1}^{x2}\vartheta(x,y,z,t)\,dxdydz \qquad (6)$$

where ϑ is MKE, EKE or BEC, and the integration limits are the coordinates delimiting the horizontal areas and the vertical layers. The 4 regions climatological time series of near surface (surface to 5m depth) MKE and EKE, are given in Fig.5.

For both WAC and Northern sub-basins, the MKE decreases from January to March, and then it gently increases until November with a relative minimum in August. Moreover the WAC region is more energetic than the Northern sub-basin. It is interesting to note that, similarly to the Poulain (2001) observations (Fig.3), in both regions a relative maximum appears in Spring and Summer. The Summer maximum occurs in September with relatively high values of

MKE and EKE. On the contrary the Spring maximum has different time occurrence: in the WAC region it appears in April and is due to MKE (EKE has low values), while in the Northern region it is observed in May with high values of both the Kinetic energy components. The MKE global maximum occurs in November for both the WAC and the Northern sub-region. On the contrary the WAC and Northern region have a very different EKE temporal behaviour. In the WAC region the EKE and MKE seasonal cycles seem to have negative correlation (see the august peak for EKE and the minimum for MKE) and the contribution of EKE to the total kinetic energy is generally smaller than 50%. In the WAC region there is no clear Po runoff related signal probably as a consequence of the extension of the region. On the contrary, in the Northern sub-basin the EKE and MKE seasonal cycles have the same temporal evolution, the May and November maxima are apparently linked to the Po runoff.

The Middle Adriatic energy cycle is correlated with both Po runoff and weakly with the wind stress work (Fig.4). The MKE and EKE values are intermediate between the Northern and Southern regions and this is clearly a transition region. The Southern sub-basin has energetic characteristics that strongly differ from the rest of the Adriatic Sea. The MKE and EKE have comparable values and similar seasonal variability of wind stress work with a well marked spring-summer minimum.

The climatological seasonal cycle of the BEC term, contained in (4), averaged for the 4 sub-regions and two different layers is shown in Fig.6. In the Northern and Middle Adriatic basins, and in the surface layer, EAPE to EKE transfer (positive BEC values) occurs in winter and from late summer to autumn. In these same regions, a possible inverse energy conversion, i.e. EKE transferred to EAPE, is observed between May and August but the values are too small to be relevant. To summarize we might say that negligible energy transfer occurs in the

Northern and Middle Adriatic regions in summer while a positive baroclinic energy transfer is realised in the remaining seasons.

In the WAC region and at the surface, the BEC is 2-3 times larger than in other regions and its temporal behaviour is similar between the WAC and the Southern region. In these two areas, the maximum of EAPE to EKE conversion occurs in summer, reaching the maximum in August. Thus the internal energy re-distribution processes reach their maximum values during summer, when the external forcings are at their minimum of intensity. The stronger mesoscales eddy field of the summer circulation has been depicted by many authors in the Mediterranean and Adriatic Sea (Artegiani *et al*., 1997b, Ayoub *et al*., 1998, Millot 1991) and here for the first time we argue that this is associated with the baroclinic energy conversion processes that are particularly active in the western intensified currents and the southern Adriatic. This might be due to the fact that these regions can accumulate EAPE during the winter that can then in turn be released to EKE. In the Adriatic, only the WAC and the Southern region (characterised by a large scale cyclonic gyre) have this capability.

Analyzing the BEC in the sub-surface layer (Fig.6) large differences are evident between the Middle and Southern Adriatic regions especially during summer time. Both time-series are always positive indicating that at this depth the energy conversion is always from EAPE to EKE. However, only the Southern Adriatic is characterized by large positive values during summer while the Middle Adriatic region reaches a minimum.

3.2 Seasonal variability and Spatial distribution of Kinetic energy

In Fig.7, 8 and 9 the MKE, EKE and BEC term monthly mean maps vertically integrated in the near-surface layer for selected months (January, May, September and November) are shown. In general the MKE and EKE monthly averaged fields show highest values in the

open sea areas of the Middle and Southern Adriatic Sea, in correspondence of the cyclonic open sea gyres characterising these regions (Artegiani *et al*., 1997b). Coastal high MKE values characterise the WAC region throughout the year with MKE two-three times larger than EKE. Other interesting features of the fields are:

1) the large MKE and EKE energy values of the Southern Adriatic region which remain high for the entire seasonal cycle;

2) the secondary maxima offshore the Gargano peninsula (Fig.1) in the EKE field, where the flow is known to be unstable and a process of barotropic/baroclinic instability of the WAC is likely to occur;

3) the high values of both MKE and EKE north and offshore the Dalmatian islands area (islands in front of Split see Fig.1);

4) the maxima of MKE and EKE across the basin between the Middle and Northern Adriatic areas, approximately along the 100-120 m bathyline (Fig.1), This area has been studied in the past and it is found to be controlled by bottom steering effects that deviate the eastern Adriatic northward flow across the basin (Carnevale *et al* 1999).

In January, the MKE and EKE (Fig.7 and 8 upper panel) show similar patterns having extended areas of high values encircling the Southern Adriatic (SAd) gyre, relative maxima along the WAC region and in the eastern side of the Middle Adriatic (MAd) gyre area. The BEC term maps (Fig.9, upper panel) indicate that EAPE is converted to EKE almost everywhere in the basin but with local maxima on the WAC region reinforcing the interpretation of baroclinic instability process being at work.

In May (Fig.7 and 8) MKE maintains high values (especially along the WAC region) while EKE reaches its minimum values. The BEC term field (Fig.9) shows at the same time a weak negative sign over the whole basin corresponding to an inverse conversion of EKE into

EAPE. Sparse maxima of baroclinic conversion (positive BEC values) are observed in the Southern branch of the WAC corresponding to local EKE maxima.

In September (Fig.7, 8 and 9) and along the WAC region the MKE, EKE are similar to the May case, but in the Southern Adriatic the maxima are mostly confined in the Western side of the basin. The BEC term instead shows large positive values off the Gargano promontory, in the northern and southern branch of the WAC. Approximately at the same location, EKE reaches the maximum values offshore the Gargano (over 180 cm^2 s^{-2}) probably due to the conversion of EAPE into EKE.

In November (Fig.7, 8 and 9) the MKE of the coastal currents is enhanced. During this season, the EKE of the WAC progressively reaches a minimum. On the contrary, in the eastern side of the basin the mesoscale energy shows an opposite trend. The branch connecting the eastern and western coastal currents of the Middle Adriatic is now characterized by high values of both EKE and MKE. The BEC field is generally positive but weak, with sparse maxima in the WAC region.

In conclusions we can say that the high values of EKE can be reasonably connected to positive values of the baroclinic conversion term in winter and summer, especially in the WAC region. In May an inverse energy exchange (EKE transformed into EAPE) seems to be at work and during autumn the energy conversion seems to be weak.

3.3 Inter-annual Variability of kinetic energy

In Fig.10 the monthly mean time series of TKE and EKE integrated between the surface and 5 meters for the whole Adriatic basin and for the 4 sub-regions (Fig.1) are shown. We show in Fig. 11 the wind work and Po runoff time series for the same time period: the wind work is maximum during late autumn and winter and it shows large events each year with an absolute

maximum in the winter 2003-2004 and autumn 2004. The Po time series is very irregular, marking the larger inter-annual variability of this forcing, the time series is characterised by large Po runoff values in 2000-2002 and lower values during the 2003-2004 period.

The energy climatological seasonal cycle discussed in the previous section is evident in the Middle and Southern Adriatic regions of Fig. 10, while the WAC and Northern Adriatic show irregular peaks in the different years. A considerable year to year variability is observed in the timing and value of the seasonal maxima and minima. Since the WAC does not show a clear repeating seasonal cycle, we argue that this is probably due to the fact that TKE and EKE are in part determined by internal energy re-distribution mechanisms as well as the Po run-off forcing which is more irregular (Fig.11).

The TKE, in all the regions except the WAC and the northern region (Fig. 10), shows maxima in late-autumn (also recovered in the climatological mean), and secondary spring and/or summer maxima, strongly affected by inter-annual and sub-regional variability. The autumn maximum is well correlated with wind stress work (Fig.11), while the other maxima seem to be a consequence of internal dynamics and Po runoff.

One of the major events observed during the simulated period is the large fresh water input started in autumn 2000 and continued during winter and spring 2001 (from October 2000 to May 2001, Fig.11). This continuous buoyancy forcing should allow for a large storage of MAPE and EAPE which can be later released through baroclinic conversion. In Fig.10 we see that, in the same period, the TKE is high in the whole Adriatic (+9% with respect with the climatological mean of the same period); this positive anomalies are enhanced in the WAC (+10%) and Southern (+20%) Adriatic region. High EKE values are present in the Northern sub-region during the first months of 2001.

The Po regime was very anomalous also during 2003, with the absence of the Spring and Autumn maxima and the runoff observed values always (except January and December) below the climatological annual mean (1500 m^3s^{-1}). The low Po runoff correlates with the smallest values of TKE and EKE observed in the overall Adriatic during Summer.

A time series maximum TKE peak is observed at the end of 2004 (Fig.10) in all the regions in correspondence with the extreme kinetic energy input event by wind stress (Fig.11). It is interesting to note that the energy input by the wind (Fig.11) is dominated in 2004 by a large number of short time scale but large amplitude events (less than 3 days). The November 2004 wind stress work monthly mean is about 1.0 N m^{-1} s^{-1} (Fig.11) but during this month episodic extreme wind events occur with a net surface energy input larger than 5 and 7 N m^{-1} s^{-1}. During this period the TKE and EKE in all the sub-basins have larger values with respect to December 2003 where the monthly wind stress work mean has similar amplitude but the episodic wind stress energy input is less extreme.

4. Summary and Conclusions

The mesoscale circulation of the Adriatic Sea and its seasonal and inter-annual variability has been investigated using a high resolution primitive equations numerical model. The model results are in good qualitative and quantitative agreement with observations (Poulain 2001; CTD and XBT observations, see Appendix-B) suggesting that an energy analysis can be carried out in order to explain some of the realistic features of the mesoscales dynamics of the basin. The basin has been subdivided in 4 regions on the basis of the kinetic energy distributions and prior knowledge of the oceanographic characteristics. This partition seems to give good results since the regions often show different characteristics.

We first have analyzed the seasonal behaviour of the MKE, EKE and the BEC (Baroclinic Energy Conversion) term. The seasonal cycle of the near-surface kinetic energy in the overall Adriatic Sea is correlated with the surface kinetic energy input deriving from the wind stress work. On the contrary the fresh water input deriving from the Po runoff input seems to affect the energy content and dynamics only in the Northern and partially in the WAC regions. The baroclinic conversion is maximum in Winter and Summer and in the WAC region it is 2-3 times larger than in the other regions. In this region, the BEC seems to be anti-correlated with the Po river inputs; in fact when the Po runoff is minimum a large amount of energy is converted from EAPE to EKE. At climatological time scales, inverse baroclinic conversions (EKE converted in EAPE) occur in Northern and Middle sub-regions. In the Middle Adriatic this process is enhanced subtracting large amount of kinetic energy from the Eddy compartment from March to August.

Moreover the seasonal EKE cycle is characterized by a large inter-annual variability. In the Northern Adriatic, the eddy field is characterized by large number of small cyclonic and anti-cyclonic structures, as shown in Fig. 12. Similar to the results obtained by Cushman-Rosin *et al.* (2007) we found that the baroclinic conversion processes occurring all along the Italian coasts produce a large number of small cyclonic and anti-cyclonic structures, which characterize the mesoscale pattern in the WAC region.

Permanent positive values of BEC index have been observed also in the Southern part of the WAC offshore the Gargano promontory (Fig.1). In this area the interaction vertical and horizontal shear, together with the complex coastline and bottom topography, generates a well defined MKE and EKE maximum in all the seasons (Fig. 7 and 8). During summer the mesoscale field is dominated by several cyclonic structures offshore the Manfredonia Gulf (Fig. 12 E and F).

The Middle Adriatic energy cycle is correlated with both the wind stress work and Po runoff time series. The MKE and EKE values are intermediate between the Northern and Southern regions indicating that this is clearly a transition region. In the surface layer, EAPE to EKE transfer occurs in winter and from late summer to autumn; while in the sub-surface layer (Fig.6) the energy conversion is always from EAPE to EKE. A MKE and EKE maxima occurs across the basin between the Middle and Northern Adriatic areas, approximately along the 100-120 m bathymetric line (Fig.7 and 8). The high EKE values of this Middle Adriatic current, connecting the eastern and western currents of the Adriatic, is related again to the development of small scale eddy structures, as shown in Fig.12.

The Southern sub-basin has energetic characteristics that strongly differ from the rest of the Adriatic Sea. The MKE and EKE have a well marked spring-summer minimum. The BEC in the surface and sub-surface layers (Fig.6) is always positive and is characterized by relatively large values also during summer. In the Southern sub-basin, most of the mesoscale dynamics is due to kinetic energy related to the SAd gyre rim current and a number of strongly variable (in terms of position and intensity) eddies dominate the mesoscale field (Fig.12).

In conclusion this work shows that the intense mesoscale dynamics of the basin is connected to external forcings, such as wind work and Po runoff, as well as internal baroclinic conversions, typical of baroclinic instability processes occurring at different intensity in the basin. The WAC and in particular its southern Adriatic region seems to be the site of the most intense energy redistribution processes in the basin. There is evidence also of inverse baroclinic energy conversions, where EKE can be transferred to EAPE, but a more consistent study of the full energy cycle is required. Another outcome of this work is the demonstration that the separation of MKE and EKE based upon a seasonal average seems to illustrate well

the characteristics of the basin cycle and could be used in the future studies to characterise the other energetic processes of the Adriatic Sea mesoscales.

Appendix-A - Kinetic Energy equations

In the following discussion pressure and density have to be considered as the dynamic pressure and density components identified in (5) as the sum of $\overline{\overline{\rho}}(x,y,z)$ and ρ'.

We start from momentum equation:

$$\frac{\partial \vec{u}}{\partial t} + \vec{u}\cdot\vec{\nabla}\vec{u} + f\vec{k}\times\vec{u} = -\frac{1}{\rho_0}\vec{\nabla}p + \vec{\nabla}\cdot\left(A_k\vec{\nabla}\vec{u}\right) \qquad \text{eq.A1}$$

to derive Kinetic energy, $K = \frac{1}{2}\left(u^2 + v^2\right)$, equations, which is obtained via scalar product of eq A.1 and $\vec{u}$:

$$\frac{\partial K}{\partial t} + \vec{u}\cdot\vec{\nabla}K = -\frac{1}{\rho_0}\vec{u}\cdot\vec{\nabla}p - \frac{g}{\rho_0}w\rho + \vec{\nabla}\cdot\left(A_k\vec{\nabla}K\right) \qquad \text{eq.A2}$$

where now the gradient operator is three-dimensional and the hydrostatic pressure equation has been used. We assume that each quantity can be divided into a mean and eddy component, $\theta = \underline{\theta} + \theta'$ and for a vector $\vec{u} = \vec{U} + \vec{u}'$. If we apply the above decomposition to each variable in eq.A1 and take the time mean, we obtain the time mean momentum equation as follows:

$$\frac{\partial \vec{U}}{\partial t} + \vec{U}\cdot\vec{\nabla}\vec{U} + f\vec{k}\times\vec{U} = -\frac{1}{\rho_0}\vec{\nabla}\underline{p} + \vec{\nabla}\cdot\left(A_k\vec{\nabla}\vec{U}\right) - \underline{\vec{u}'\cdot\vec{\nabla}\vec{u}'} \qquad \text{eq.A3}$$

Subtracting eq.A3 to eq.A1 we obtain the momentum equation for the eddy field:

$$\frac{\partial \vec{u}'}{\partial t} + \vec{U}\cdot\vec{\nabla}\vec{u}' + f\vec{k}\times\vec{u}' = -\frac{1}{\rho_0}\vec{\nabla}p' + \vec{\nabla}\cdot\left(A_k\vec{\nabla}\vec{u}'\right) + \underline{\vec{u}'\cdot\vec{\nabla}\vec{u}'} - \vec{u}'\cdot\vec{\nabla}\vec{u}' - \vec{u}'\cdot\vec{\nabla}\vec{U} \qquad \text{eq.A4}$$

The equation for mean kinetic energy, $MK = \frac{1}{2}\rho_0\left(U^2 + V^2\right)$, and eddy kinetic energy, $EK = \frac{1}{2}\rho_0\left(u'^2 + v'^2\right)$, are obtained by multiplying eq.A3 by $\vec{U}$ and eq.A4 by $\vec{u}'$:

$$\underset{(1M)}{\frac{\partial MK}{\partial t}} + \underset{(2M)}{\vec{U}\cdot\vec{\nabla}MK} = \underset{(3M)}{-\vec{U}\cdot\vec{\nabla}\underline{p}} \underset{(4M)}{- g\underline{w}\underline{\rho}} + \rho_0\left[\underset{(5M)}{-\vec{U}\cdot\left(\underline{\vec{u}'\cdot\vec{\nabla}\vec{u}'}\right)} + \underset{(6M)}{\vec{\nabla}\cdot\left(A_k\vec{\nabla}MK\right)}\right]$$

and

$$\underset{(1E)}{\frac{\partial EK}{\partial t}} + \underset{(2E1)}{\vec{U}\cdot\vec{\nabla}EK} + \underset{(2E2)}{\vec{u}'\cdot\vec{\nabla}EK} = \underset{(3E)}{-\vec{u}'\cdot\vec{\nabla}p'} \underset{(4E)}{- gw'\rho'} + \rho_0\left[\underset{(5E1)}{-\vec{u}'\cdot\left(\vec{u}'\cdot\vec{\nabla}\vec{U}\right)} + \underset{(5E2)}{\vec{u}'\cdot\left(\underline{\vec{u}'\cdot\vec{\nabla}\vec{u}'}\right)} + \underset{(6E)}{\vec{\nabla}\cdot\left(A_k\vec{\nabla}EK\right)}\right]$$

Where:

1M and 1E are the local tendency. Depending on the definition of the mean field 1M could be zero;

2M and 2E1 are the advection by the mean flow;

2E2 is the advection by the eddy flow;

3M and 3E are the horizontal pressure work;

4M and 4E are the vertical pressure work (conversion to APE). The same quantities appear in the equation of available potential energy (both eddy and mean);

5M and 5E1 are the energy conversion by the Reynolds stresses (EK to MK and vice versa). The 5E1 term need to be properly averaged;

5E2 is the net conversion from eddy to first order correlation. The first order correlation is define as the mixed produce of mean and eddy field;

6M and 6E are dissipation rates.

Appendix-B: Model Validation

In this appendix we present a model-data comparison. Three different data-set have been used for model validation: CTD data, SeaWIFS chlorophyll concentration images and XBT data. The first data-set derives from NATO (Naval Undersea Research Centre of La Spezia) CTD cruises in Adriatic Sea during January-February 2001, September-October 2002 and April-May 2003. The second and the third dataset have been collected within the ADRICOSM (ADRIatic sea integrated COastal areaS and river basin Management system; *www.bo.ingv.it/adricosm*) project. Satellite images are obtained with a space objective interpolation scheme (Santoleri *et al*., 1991) on a regular horizontal grid. Expendable Bathythermograph (XBT) temperature profiles were collected as part of the ADRICOSM monitoring program for the open ocean areas of the southern Adriatic by means of Voluntary Observing Ships (VOS).

The comparison with the CTD data is shown in term of T/S diagrams. The data have been divided according to time (years) and geographical positions: North, Middle and Southern Adriatic. In Fig.13 the results of such procedure are shown. In the Northern sub-basin the model is affected by a temperature negative bias particularly evident during 2001. Good agreement is observed between model predicted and observed salinity. The temperature negative bias disappears in the Middle and Southern regions, moreover in these areas model results are characterised by salinity underestimation. In general the model does not show a significant drift from year to year and seems able to reproduce the observed inter-annual variability.

In Fig.14 a comparison between XBT data and model predicted temperature is shown. In the upper sub-panel the surface elevation field for Jun-5-2003 together with the sampling position

(dark dots) are shown. In the other two sub-plots the temperature anomaly sections from observation and model results are shown. The model predicted thermocline is too shallows and the horizontal structures too week, moreover a remarkable agreement can be found between the positions of the small cyclonic and anti-cyclonic structure. The most evident signal in the XBT data is an anti-cyclonic gyre in the middle of the section detected as a deepening of the thermocline (from 20 to 40m depth, Lon 17.4). The same structure is present in the model solution, both in surface elevation field and anomaly temperature section, but are weaker. In the surface elevation a clear positive core is observed along the XBT track indicating an anti-cyclonic gyre. In the temperature anomaly section the same signal appears with a deepening of the simulated thermocline (from 10 to 20m depth).

When considered as quasi-passive tracers, satellite visible data can be used to explore the circulation dynamics (Barale et al 1986, Mauri and Poulain 2001). Here in order to validate the model simulated dimension and distribution of the eddies along the WAC region, a comparison between SeaWIFS chlorophyll concentration data and model predicted surface salinity has been carried out.

In Fig.15 this comparison for May 4 2003 is shown. With the only exception of the Northern Adriatic, where the presence of the Po river, with its large load of nutrients strongly affect the chlorophyll concentration, the SeaWIFS maps can be considered a good indicator of the small circulation features. Good agreement can be noted between positions and dimensions of modelled and observed structures. Particularly good seems the model capacity to reproduce the small filaments and gyre appearing from Middle Adriatic to the area south of Gargano peninsula.

References

Ayoub N, Le Traon PY, De Mey P. A description of the Mediterranean surface variable circulation from combined ERS-1 and TOPEX/POSEIDON altimetric data Journal of Marine Systems, Volume 18, Issues 1-3, 1998, pp 3-40

Artegiani A, Pariante R, Paschini E, Russo A, Totti C. Seasonal evolution of the physical water properties observed from the Senigallia transect. In: Hopkins, T.S. et al. Eds., The Adriatic Sea. Ecosystem Report, vol. 32, European Commission, Brussels, 1999. pp. 59–70EUR 18834.

Artegiani A, Bregant D, Paschini E, Pinardi N, Raicich F, Russo A. The Adriatic Sea general circulation. Part I: Air sea interaction and water mass structure. J Phys Oceanogr 1997; 27: 1492-1514 a.

Artegiani A, Bregant D, Paschini E, Pinardi N, Raicich F, Russo A. The Adriatic Sea general circulation. Part II: Baroclinic circulation structure. J Phys Oceanogr 1997; 27: 1515-1532 b.

Barale V, McClain CR, Malanotte-Rizzoli P. Space and time variability of the surface color field in the northern Adriatic Sea, *J. Geophys. Res.*,1986: **91**, 12957-12974.

Bergamasco A, Gacic M, Boscolo R, Umgiesser G. Winter oceanographic conditions and water mass balance in the Northern Adriatic (February 1993), J Mar Sys,1996: 7, 67-94.

Blumberg AF, Mellor GL. A description of a three-dimensional coastal ocean circulation model. In: Heaps NS editor. Three-dimensional coastal ocean models, American Geophysical Union, Washington D.C., 1987; 208 pp.

Carnevale GF, Llewellyn Smith SG, Crisciani F, Purini R, Serravall R. Bifurcation of a coastal current at an escarpment. J. Phys. Oceanogr. 1999; 29, 969–985

Chiggiato J, Zavatarelli M, Castellari S, Deserti M. Interannual variability of surface heat fluxes in the Adriatic Sea in the period 1998-2001 and comparison with observation. Sci Total Environ 353, Issue 1-3, 2005; 89-102

Cushman-Roisin B, Korotenko KA, Galos CE, Dietrich DE. Simulation and characterization of the Adriatic Sea mesoscale variability, J. Geophys. Res., 112, 2007; C03S14, doi:10.1029/2006JC003515.

Estubier A., and Lévy M. Quel schéma numérique pour le transport d'organismes biologiques par la circulation océanique. Note Techniquesdu Pôle de modélisation, Institut Pierre-Simon Laplace ;2000 : 81pp.

Harrison D.E. and A.R. Robinson: Energy analysis of open regions of turbulent flows: mean eddy energetics of a numerical ocean circulation experiment. *Dyn. Atmos. Oceans*; 1978: 2, 185-211.

Hopkins TS, Artegiani A, Kinder C, Pariante R.. A discussion of the northern Adriatic circulation and flushing as determined from the ELNA hydrography. In: Hopkins, T.S. et al. Eds. , The Adriatic Sea. Ecosystem Report, vol. 32, European Commission, Brussels;1999: pp. 85–106EUR 18834.

Jochum M., Malanotte-Rizzoli P., Busalacchi A.. Tropical instability waves in the Atlantic Ocean. Ocean Modelling 2004, 7: 145–163

Legates, D. R. and C. J. Wilmott. Mean seasonal and spatial variability in a gauge corrected global precipitation. Int. J. Climatol. 1990, 10: 121-127.

Lorenz EN. Available potential energy and the maintenance of the general circulation. *Tellus*, 1955; **7**, 157–167

Masina S, Pinardi N. Mesoscale data assimilation studies in the middle Adriatic Sea. Continental Shelf Research 1994: 14, No. 12: 1293-1310.

Mantziafou A, Lascaratos A. An eddy resolving numerical study of the general circulation and deep-water formation in the Adriatic Sea. Deep-Sea Research I 2004; 51: 921–952.

Mauri E, Poulain PM. Northern Adriatic Sea surface circulation and temperature/pigment fields in September and October 1997, J. Mar. Syst. 2001, 29, 51– 67.

Millot C. Mesoscale and seasonnal variabilities of the circulation in the western Mediterranean, Dyn. Atm. Oceans 1991, 15, 179-214.

Oddo P, Pinardi N, Zavatarelli M. A numerical study of the interannual variability of the Adriatic Sea (2000-2002). Science of the Total Environment; 353, 2005;39-56.

Oddo, P., Pinardi, N., Zavatarelli, M., and Coluccelli, A.: The Adriatic Basin Forecasting System, Acta Adriatica, 47 (Suppl.), 169-184, 2006.

Orlanski I, Katzfey J. The life Cycle of a Cyclone Wave in the Southern Hemisphere. Part I: Eddy Energy Budget. Journal of the Atmospheric Sciences 1991: 48 (17); 1972-1998 pp.

Paschini E, Artegiani A, Pinardi N. The mesoscale eddy field of the middle Adriatic during fall 1988. Deep-Sea Res. 1993 I, 40, 1365–1377.

Pedlosky J,. *Geophysical Fluid Dynamics*, 2nd Edition. Springer-Verlag, New York, 1987; 710 pp.

Poulain PM, Adriatic Sea surface circulation as derived from drifter data between 1990 and 1999. JMS,:2001:29, 12-32

Provini A, Crosa G, Marchetti R. Nutrient export from the Po and Adige river basin over the last 20 years. Sci Total Environ 1992; suppl.: 291-313.

Pullen J, Doyle J, Hodur R, Ogston A, Book J, Perkins H, Signell R. Coupled ocean-atmosphere nested modeling of the Adriatic Sea during winter and spring 2001. Journal of Geophysical Research 2003; 108(C10), 3320, doi:10.1029/2003JC001780

Pullen J, Doyle J, Signell R. Two-way air-sea coupling: A study of the Adriatic. Monthly Weather Review 2006; 134(5), 1465–1483

Raicich F. Note on flow rates of the Adriatic rivers, Istituto Talassografico Sperimentale Trieste. Technical Report 1994; RF02: 94, 8.

Santoleri R, Marullo S and Bohm E. An objective analysis scheme for AVHRR imagery. Int. J. Remote Sens.,1991; 12 (4): 681-693.

Tonani M, Pinardi N, Dobricic S, Pujol I, Fratianni C. A high resolution free surface model of the Mediterranean Sea. Ocean Sci. Discuss. 2007; 4, 213-244.

Ursella, L., P.-M. Poulain, and R. P. Signell (2006), Surface drifter derived circulation in the northern and middle Adriatic Sea: Response to wind regime and season, J. Geophys. Res., 111, C03S04, doi:10.1029/2005JC003177. [printed 112(C3), 2007]

Zavatarelli M, Pinardi N, Kourafalou VH, Maggiore A. Diagnostic and prognostic model studies of the Adriatic Sea circulation. Seasonal variability. J Geophys Res 2002; 107(C1), art 3004.

Zavatarelli M, Pinardi N. The Adriatic Sea Modelling System: a nested Approach. Ann Geophysicae 2003; 21: 345-364.

Figure Captions

Fig.01 The Adriatic Sea bathymetry and high resolution coastlines. The coloured areas denote the sub-basins areas where diagnostics are calculated: WAC region [WR], Northern [NR], Middle [MR] and Southern Adriatic region [SR].

Fig.02 Mean surface Adriatic circulation for (A) summer and (B) winter (season definition according Artegiani *et al*. 1997). The mean has been computed averaging the daily surface current from 2000 to 2004.

Fig.03 Time series of monthly mean TKE (MKE+EKE) from the 1999-2004 model simulation (dashed line) and from 1990-1999 lagrangian observations (Poulain, 2001, solid line). Unit are $cm^2\ s^{-2}$.

Fig.04 Time series of wind stress work ($N\ s^{-1}\ m^{-1}$, upper panel) and Po river runoff ($m^3\ s^{-1}$ lower panel). The data have been averaged from 1-Jan-1999 to 31-Dec-2004.

Fig.05 Time series of near surface (0 to 5 m depth) climatological MKE (solid line) and EKE (dashed line) for the sub-regions reported in Fig.01. Unit are $cm^2\ s^{-2}$**.**

Fig.06 **(**Upper panel) Time series of vertical integrated (5-15 m) climatological BEC indicator for the 4 sub-regions reported in Fig.01. (Lower panel) Time series of vertical integrated (15-100m) climatological BEC indicator for the Middle and Southern Adriatic Regions (Fig.01). Units are $J\ s^{-1}\ m^{-3}$**.**

Fig.07 Monthly Mean maps of MKE averaged over the first 5m. Area whit MKE larger than 80 $cm^2\ s^{-2}$ are shaded. Units are $cm^2\ s^{-2}$**.**

Fig.08 Monthly Mean maps of EKE averaged over the first 5m. Area whit EKE larger than 80 $cm^2\ s^{-2}$ are shaded. Units are $cm^2\ s^{-2}$**.**

Fig.09 Monthly Mean maps of BEC indicator integrated from 5-15 m depth. Positive values indicate energy transfer from Eddy Available Potential Energy to EKE. Units are $J\ s^{-1}\ m^{-3}$**.**

Fig.10 Time series of: monthly TKE (solid lines with + markers) and EKE (dashed lines with circle markers) horizontally and vertically averaged (from surface to 5m). The horizontal mean has been computed over the regions reported in Fig.01. Units are $cm^2\ s^{-2}$**.**

Fig.11 Time series of wind stress work ($N\ s^{-1}\ m^{-1}$, upper panel) and Po river runoff ($m^3\ s^{-1}$ lower panel). In the wind stress work time panel filled markers indicate monthly mean, unfilled markers indicate daily values larger than 1 $N\ s^{-1}\ m^{-1}$.

Fig.12 Examples of Mean (tick arrows) and Eddy (thin arrow) near-surface (2m) surface circulation defined according (3). **(A)** Northern Adriatic 31-Jul-2001. **(B)** Northern Adriatic 21-Nov-2003. **(C)** Middle Adriatic 15-Jun-2003. **(D)** Middle Adriatic 21-Nov-2003. **(E)** Southern Adriatic 31-Jul-2001. **(F)** Southern Adriatic 15-Jun-2003. In all the subplot Mean field has been sub-sampled.

Fig.13 T-S diagrams from observations (dark dots) and model output (red dots) for years 2001 (A) 2002 (B) and 2003 (C).

Fig.14 (Upper panel) Surface Elevation daily mean from model output for 2003-05-06**.** Also the XBT stations positions are shown. In the middle and bottom panels the vertical section of observed and simulated temperature anomaly along the XBT track are reported (°C).

Fig.15 Comparison between Satellite Chlorophyll from SeaWIFS (Courtesy of Lia Santoleri, GOS-CNR, Rome, Italy) and model predicted sea surface salinity for May 4, 2003.

FIGURES

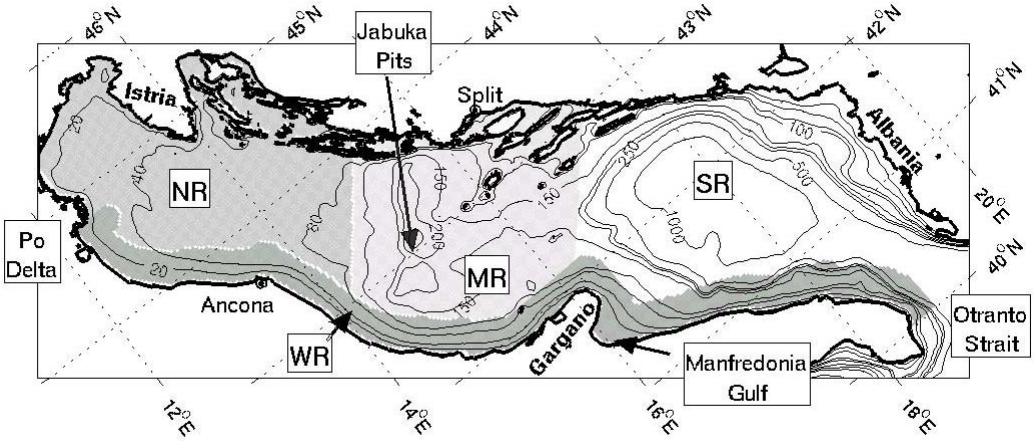

Fig.01 The Adriatic Sea bathymetry and high resolution coastlines. The coloured areas denote the sub-basins areas where diagnostics are calculated: WAC region [WR], Northern [NR], Middle [MR] and Southern Adriatic region [SR].

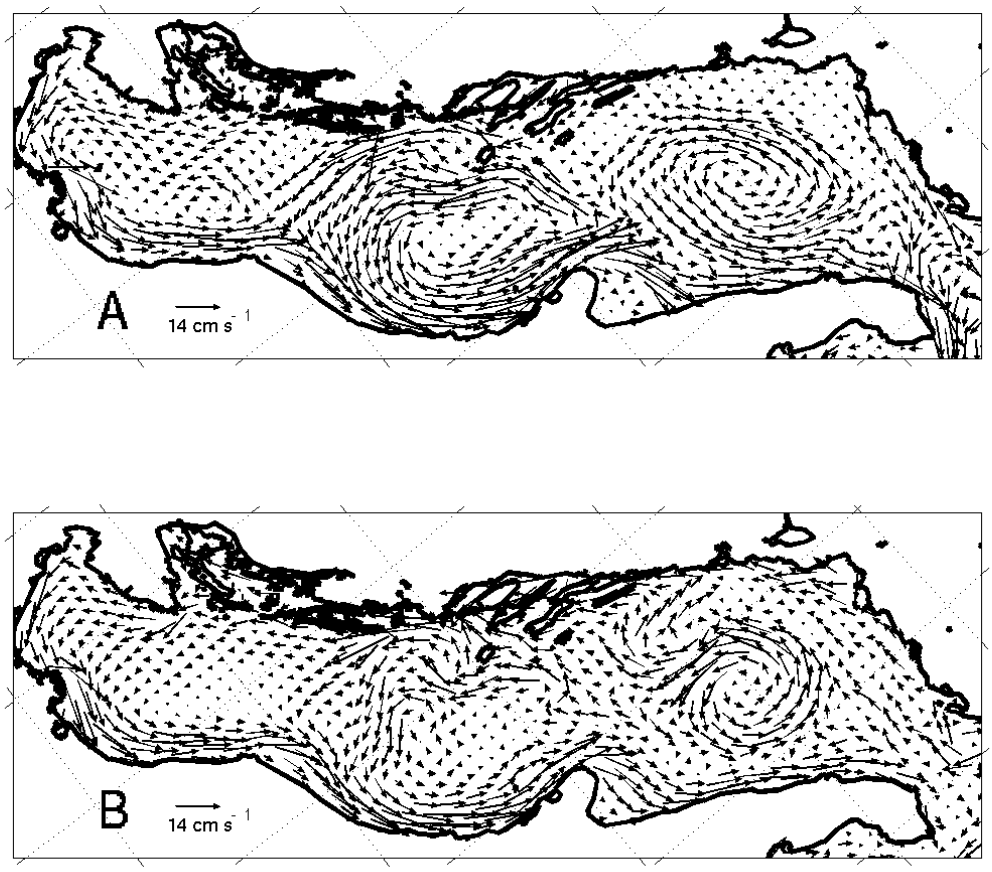

Fig.02 Mean surface Adriatic circulation for (A) summer and (B) winter (season definition according Artegiani *et al*. 1997). The mean has been computed averaging the daily surface current from 2000 to 2004.

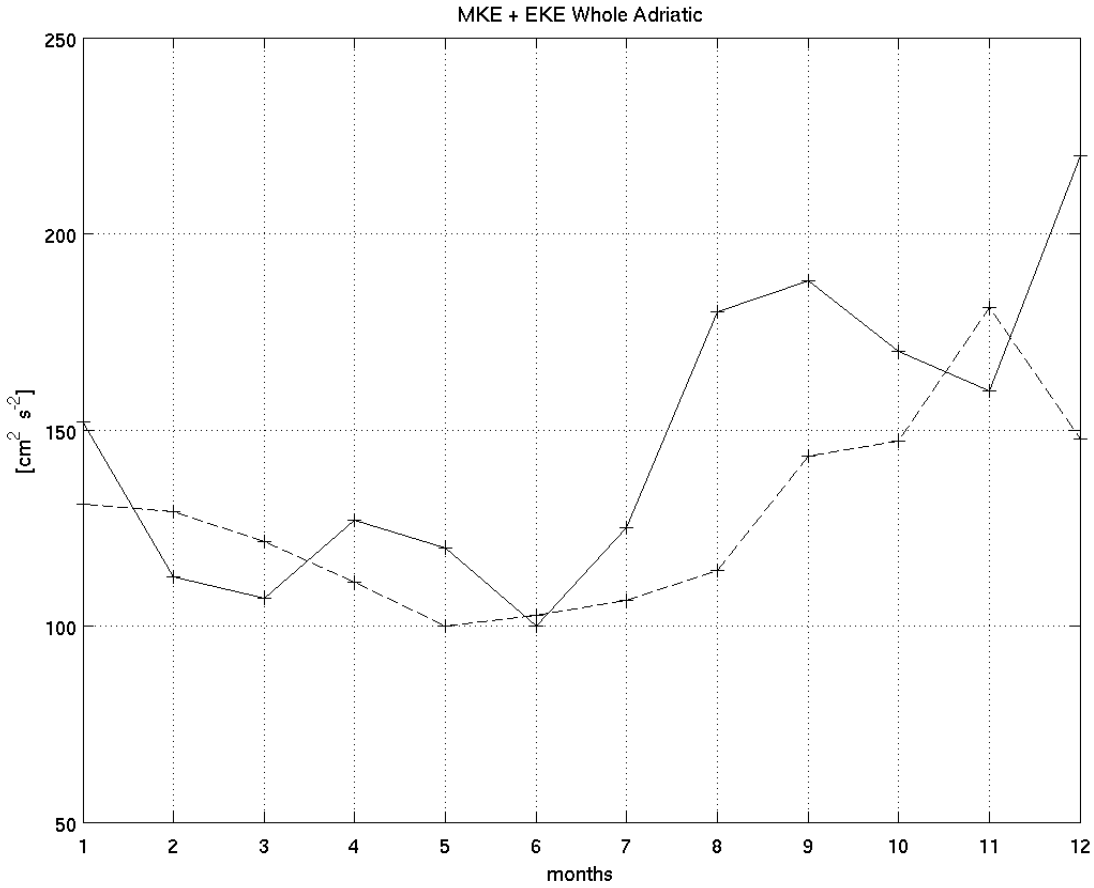

Fig.03 Time series of monthly mean TKE (MKE+EKE) from the 1999-2004 model simulation (dashed line) and from 1990-1999 lagrangian observations (Poulain, 2001, solid line). Unit are $cm^2\ s^{-2}$.

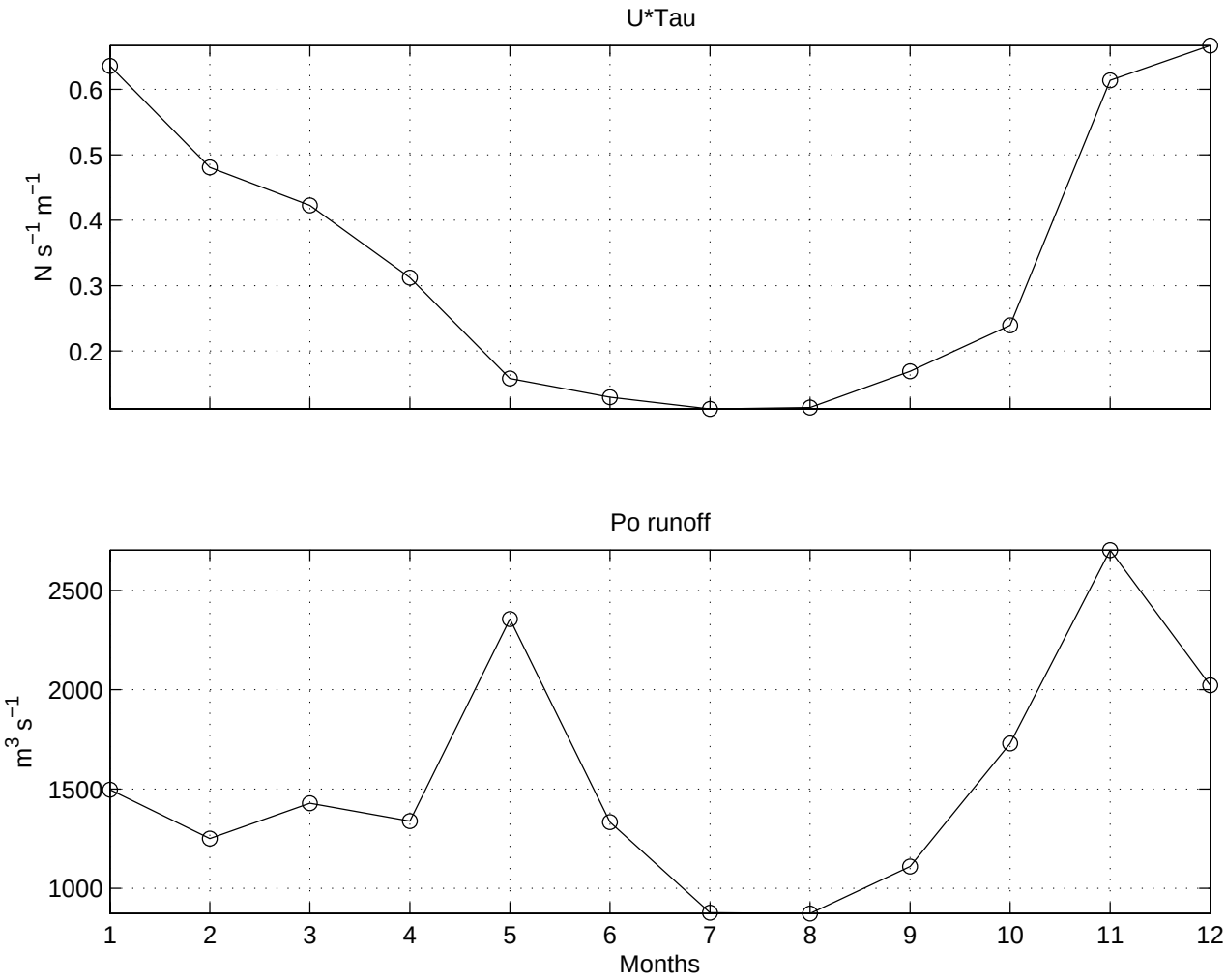

Fig.04 Time series of wind stress work (N s^{-1} m^{-1}, upper panel) and Po river runoff (m^3 s^{-1} lower panel). The data have been averaged from 1-Jan-1999 to 31-Dec-2004.

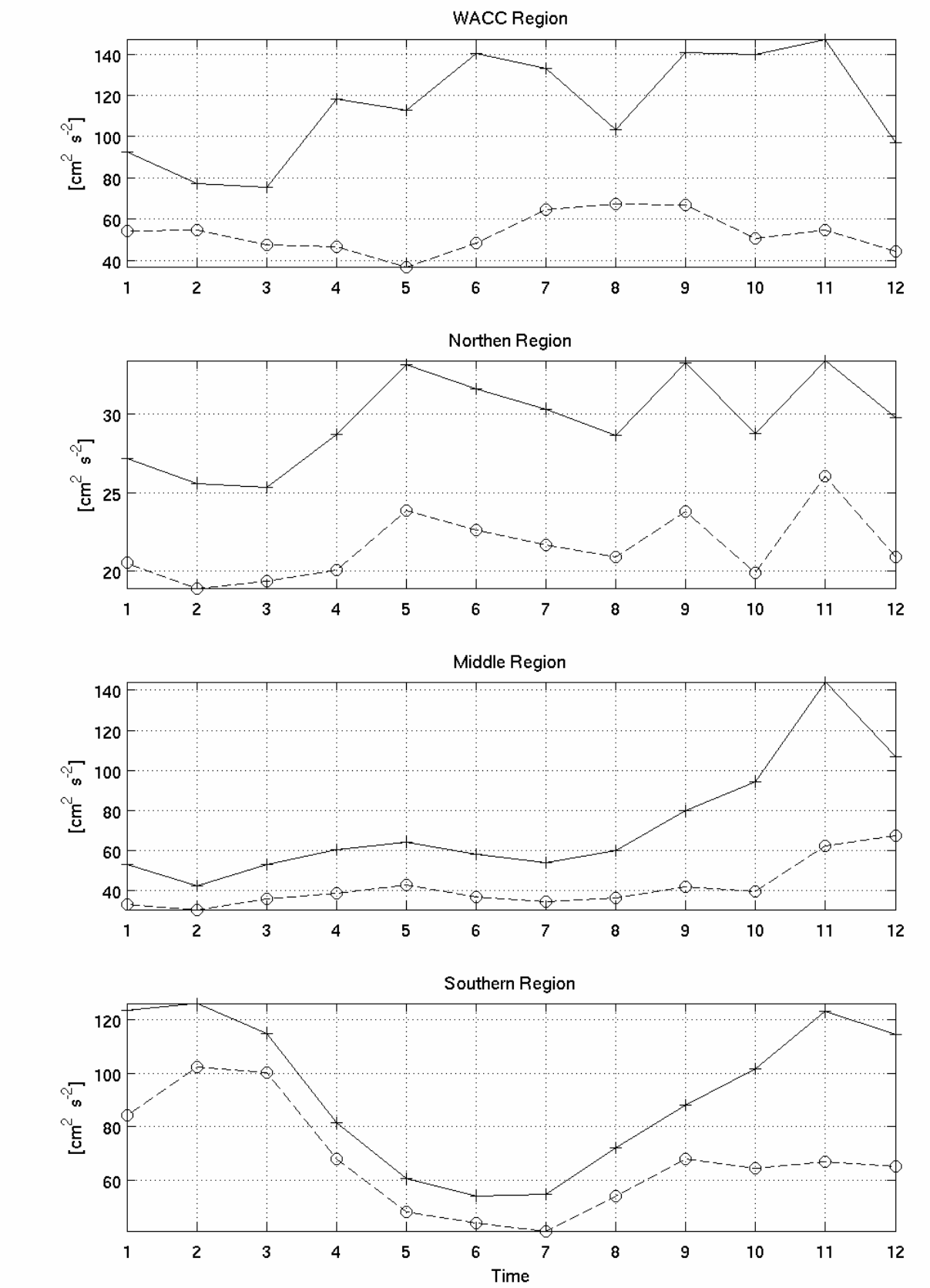

Fig.05 Time series of near surface (0 to 5 m depth) climatological MKE (solid line) and EKE (dashed line) for the sub-regions reported in Fig.01. Unit are $cm^2\ s^{-2}$**.**

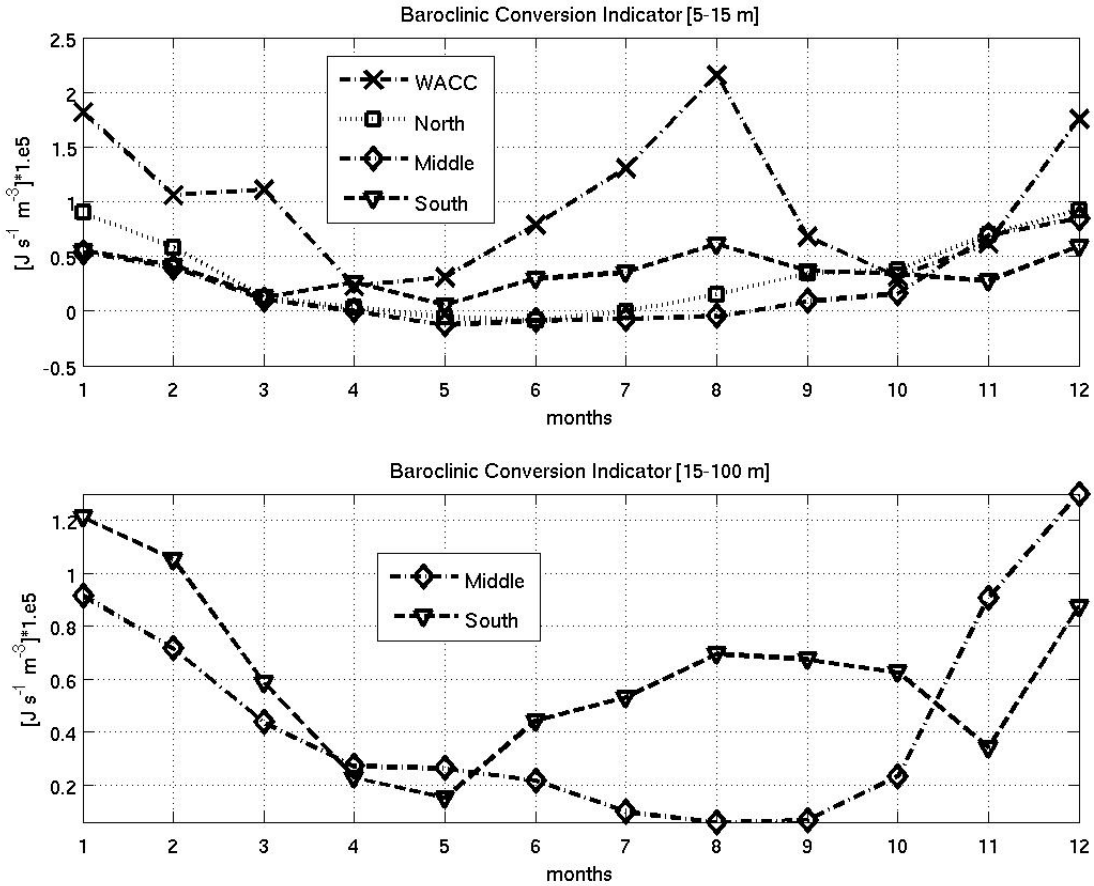

Fig.06 **(**Upper panel) Time series of vertical integrated (5-15 m) climatological BEC indicator for the 4 sub-regions reported in Fig.01. (Lower panel) Time series of vertical integrated (15-100m) climatological BEC indicator for the Middle and Southern Adriatic Regions (Fig.01). Units are J s^{-1} m^{-3}**.**

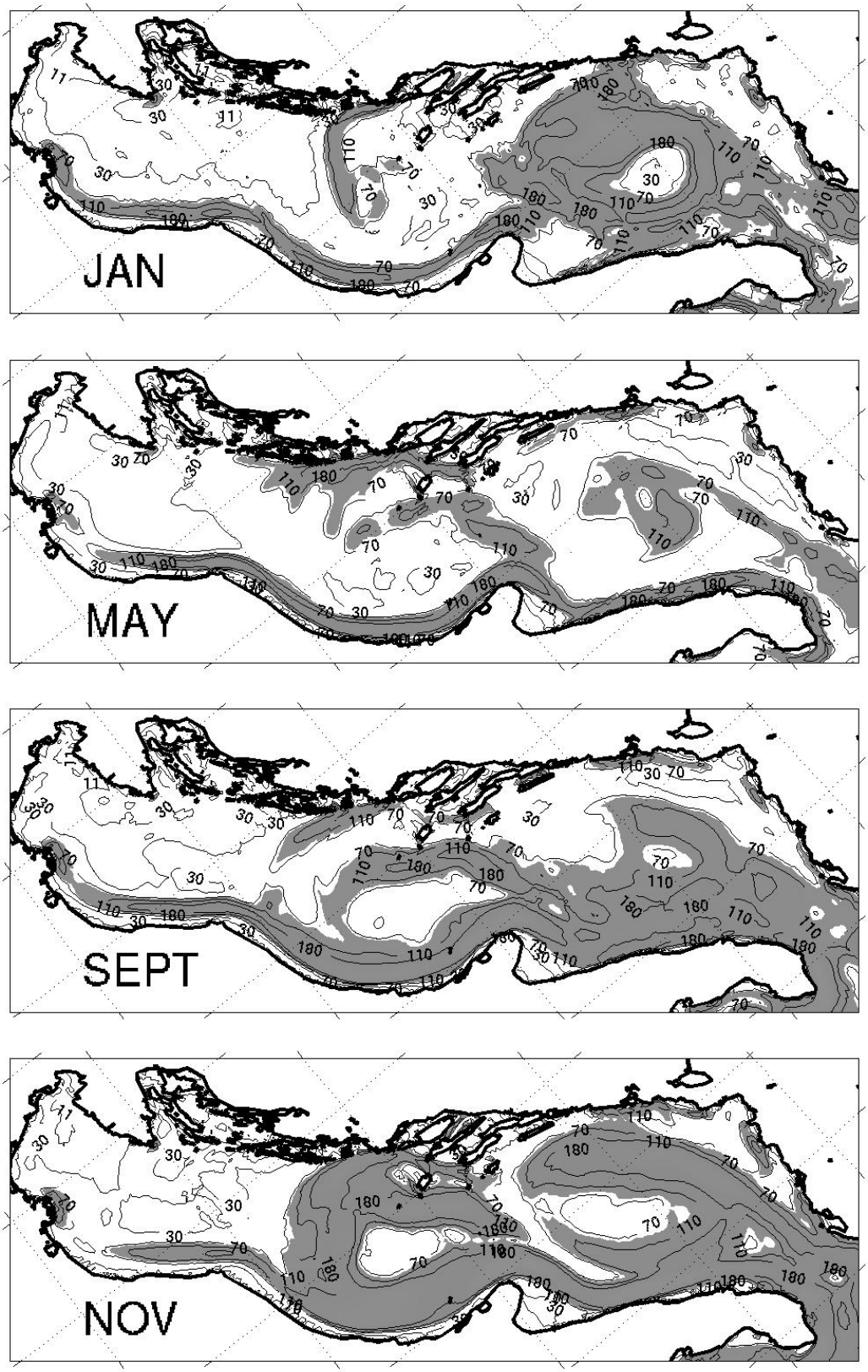

Fig.07 Monthly Mean maps of MKE averaged over the first 5m. Area whit MKE larger than 80 $cm^2\ s^{-2}$ are shaded. Units are $cm^2\ s^{-2}$**.**

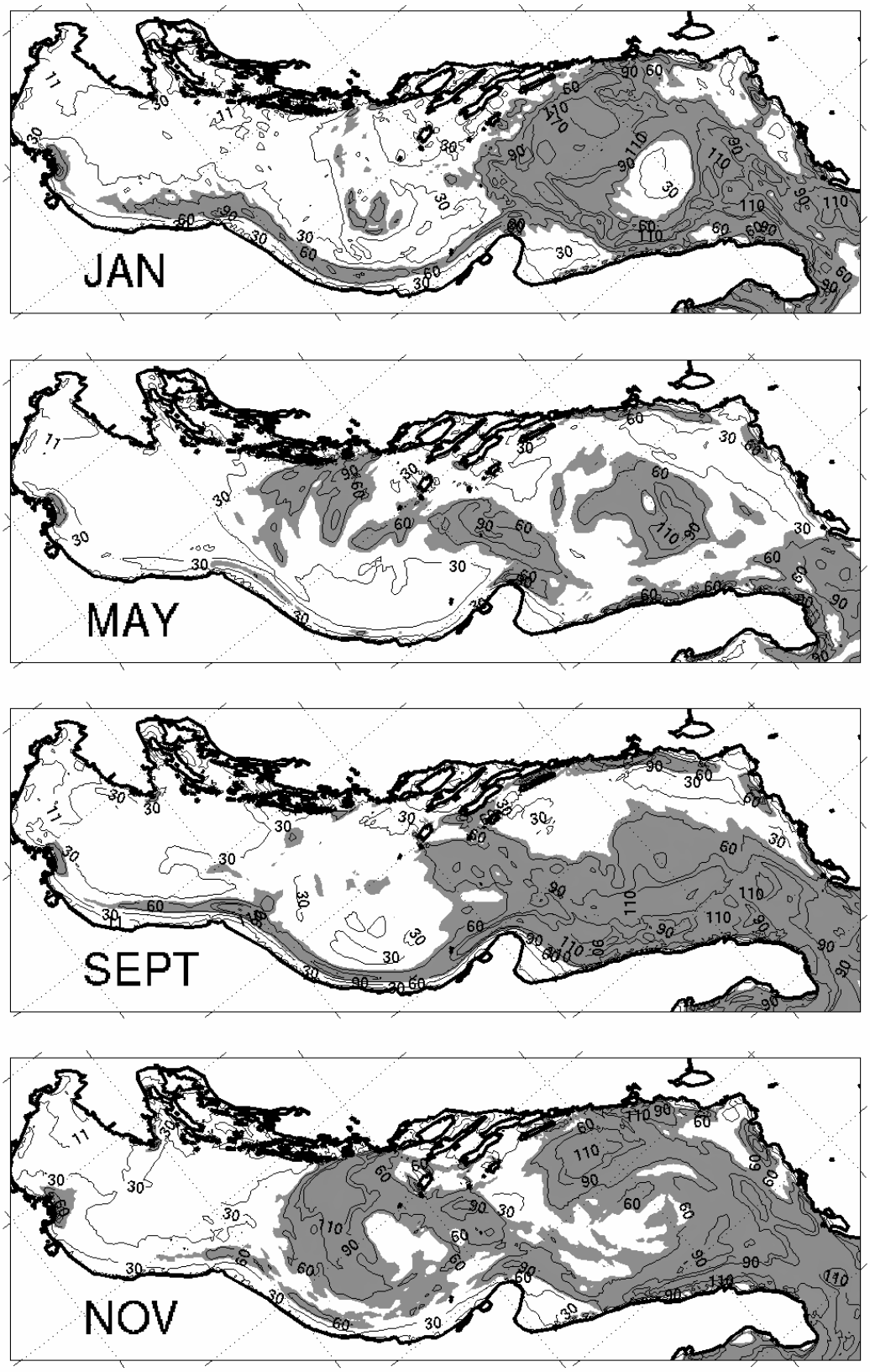

Fig.08 Monthly Mean maps of EKE averaged over the first 5m. Area whit EKE larger than 80 $cm^2\ s^{-2}$ are shaded. Units are $cm^2\ s^{-2}$**.**

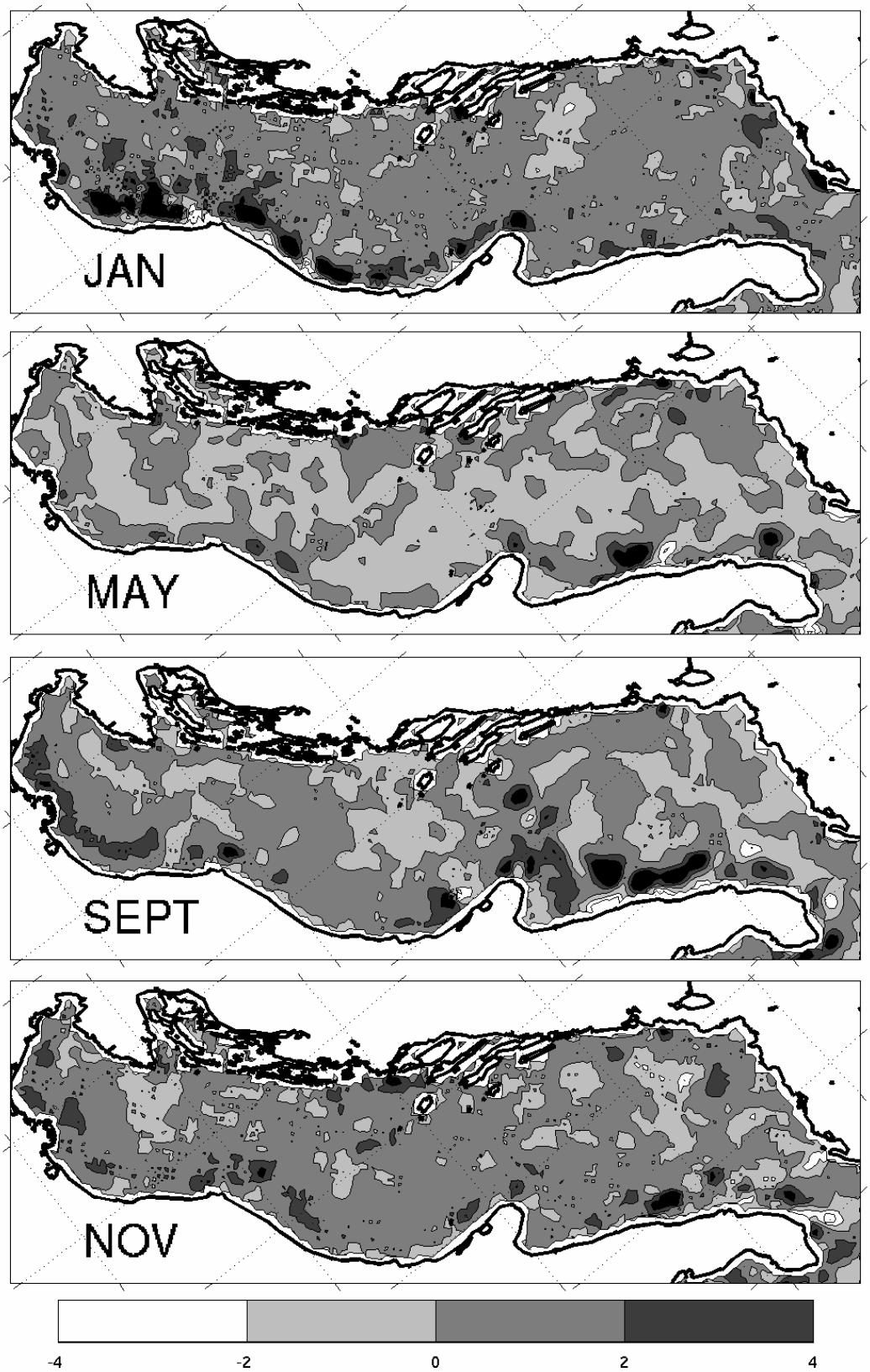

Fig.09 Monthly Mean maps of BEC indicator integrated from 5-15 m depth. Positive values indicate energy transfer from Eddy Available Potential Energy to EKE. Units are J s^{-1} m^{-3}**.**

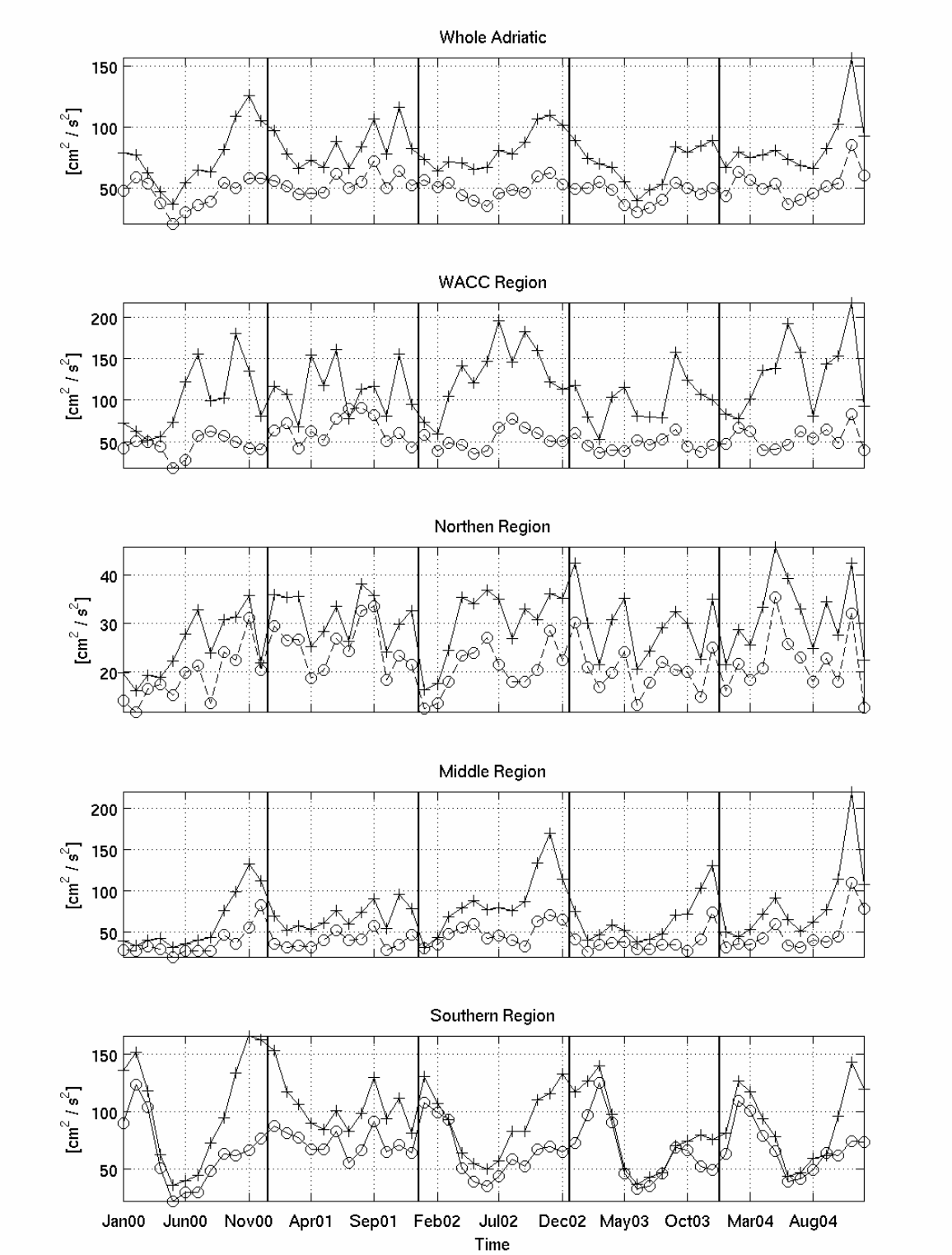

Fig.10 Time series of: monthly TKE (solid lines with + markers) and EKE (dashed lines with circle markers) horizontally and vertically averaged (from surface to 5m). The horizontal mean has been computed over the regions reported in Fig.01. Units are $cm^2\ s^{-2}$**.**

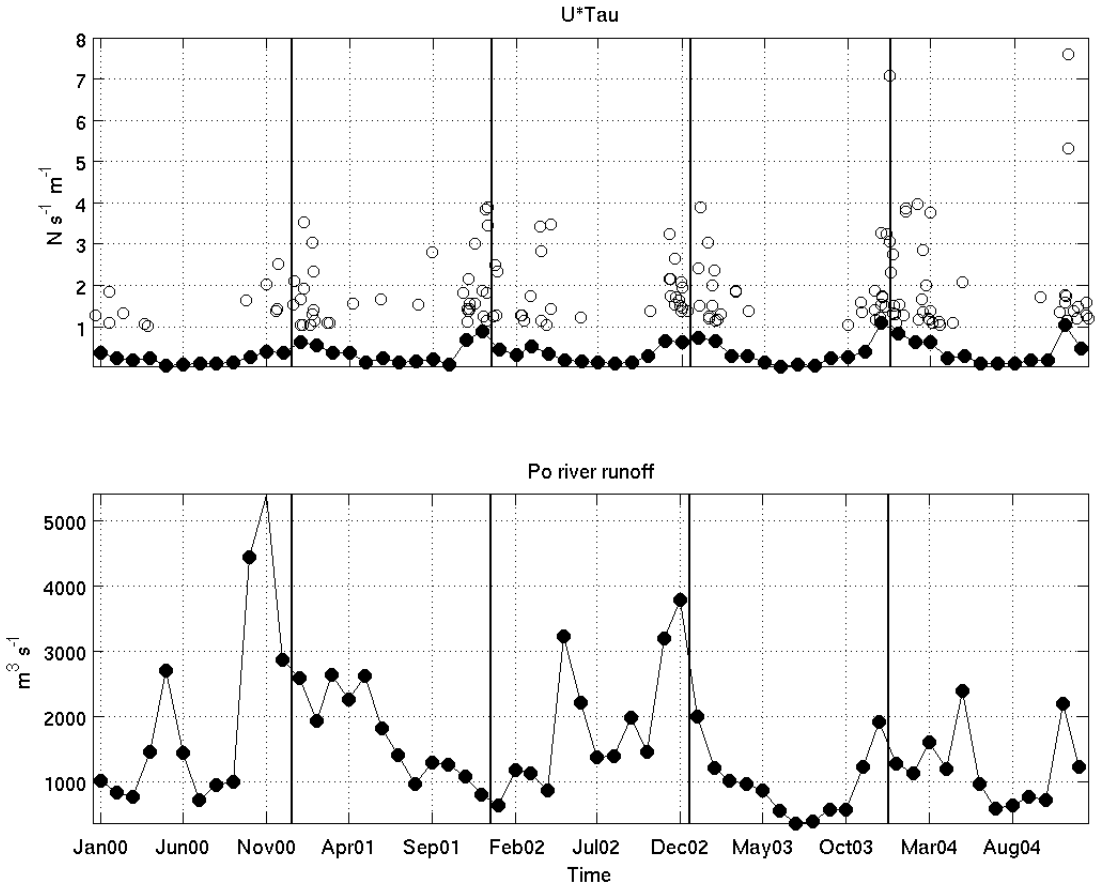

Fig.11 Time series of wind stress work (N s^{-1} m^{-1}, upper panel) and Po river runoff (m^3 s^{-1} lower panel). In the wind stress work time panel filled markers indicate monthly mean, unfilled markers indicate daily values larger than 1 N s^{-1} m^{-1}.

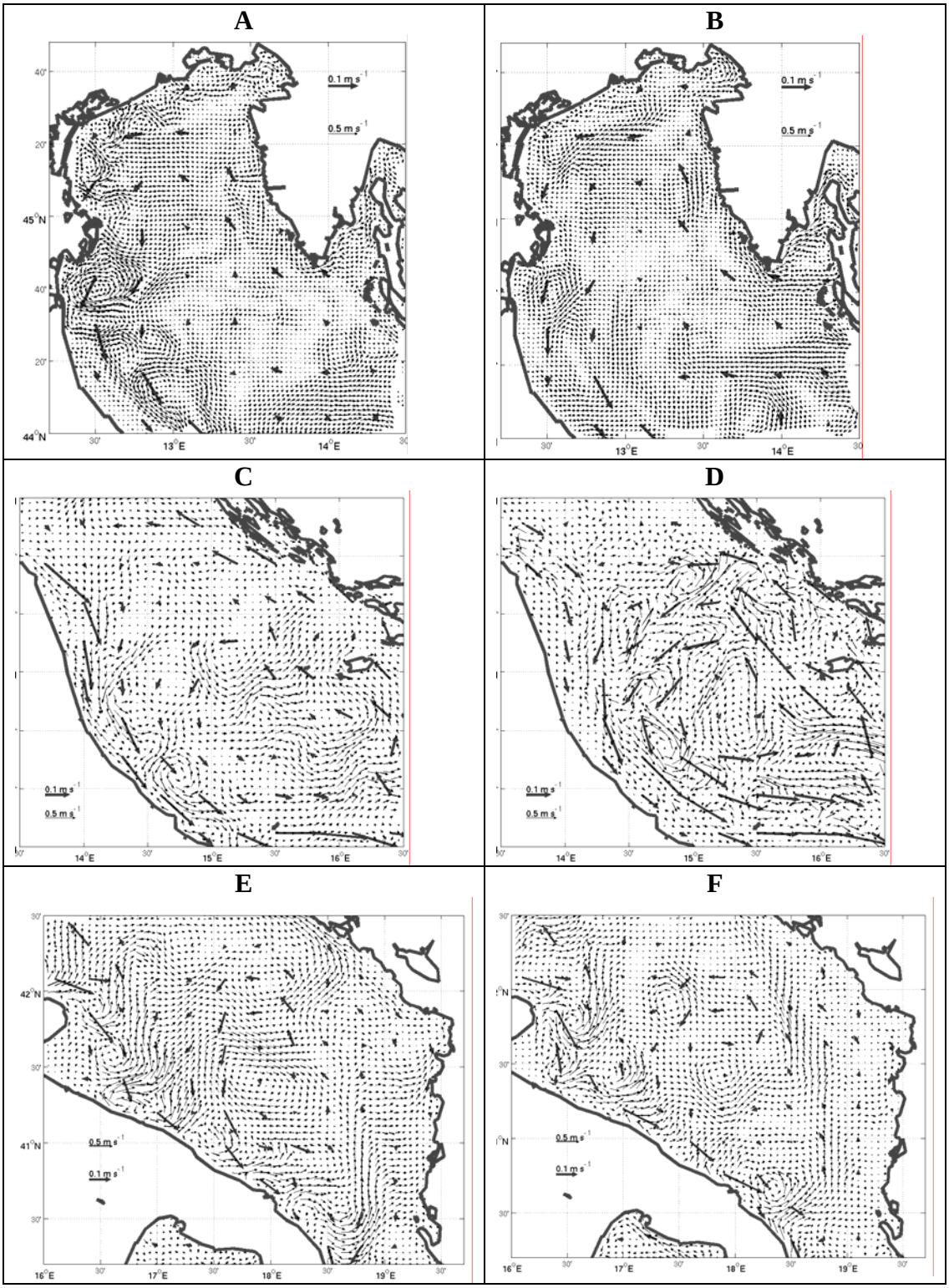

Fig.12 Examples of Mean (tick arrows) and Eddy (thin arrow) near-surface (2m) surface circulation defined according (3). **(A)** Northern Adriatic 31-Jul-2001. **(B)** Northern Adriatic 21-Nov-2003. **(C)** Middle Adriatic 15-Jun-2003. **(D)** Middle Adriatic 21-Nov-2003. **(E)** Southern Adriatic 31-Jul-2001. **(F)** Southern Adriatic 15-Jun-2003. In all the subplot Mean field has been sub-sampled.

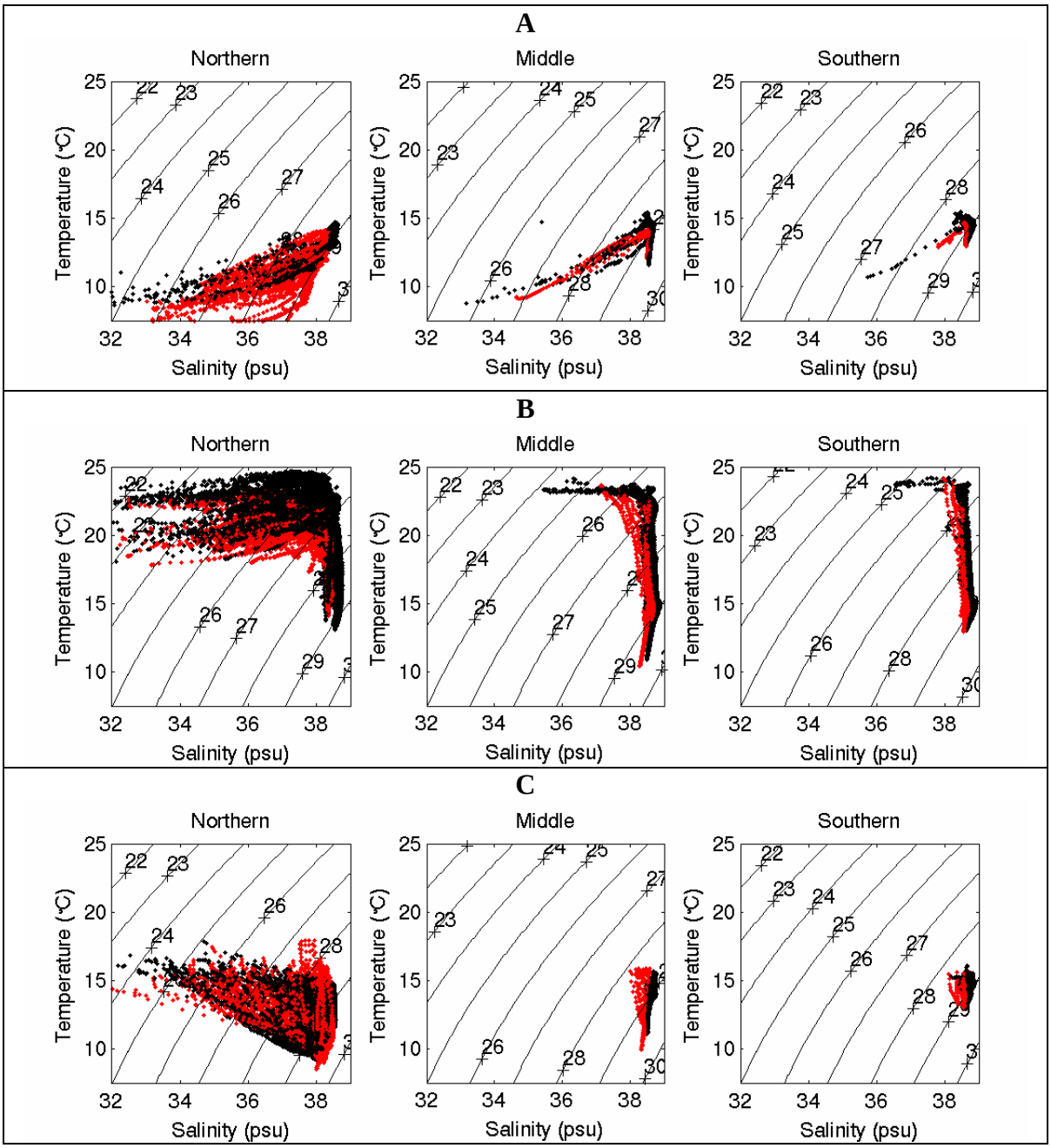

Fig.13 T-S diagrams from observations (dark dots) and model output (red dots) for years 2001 (A) 2002 (B) and 2003(C)..

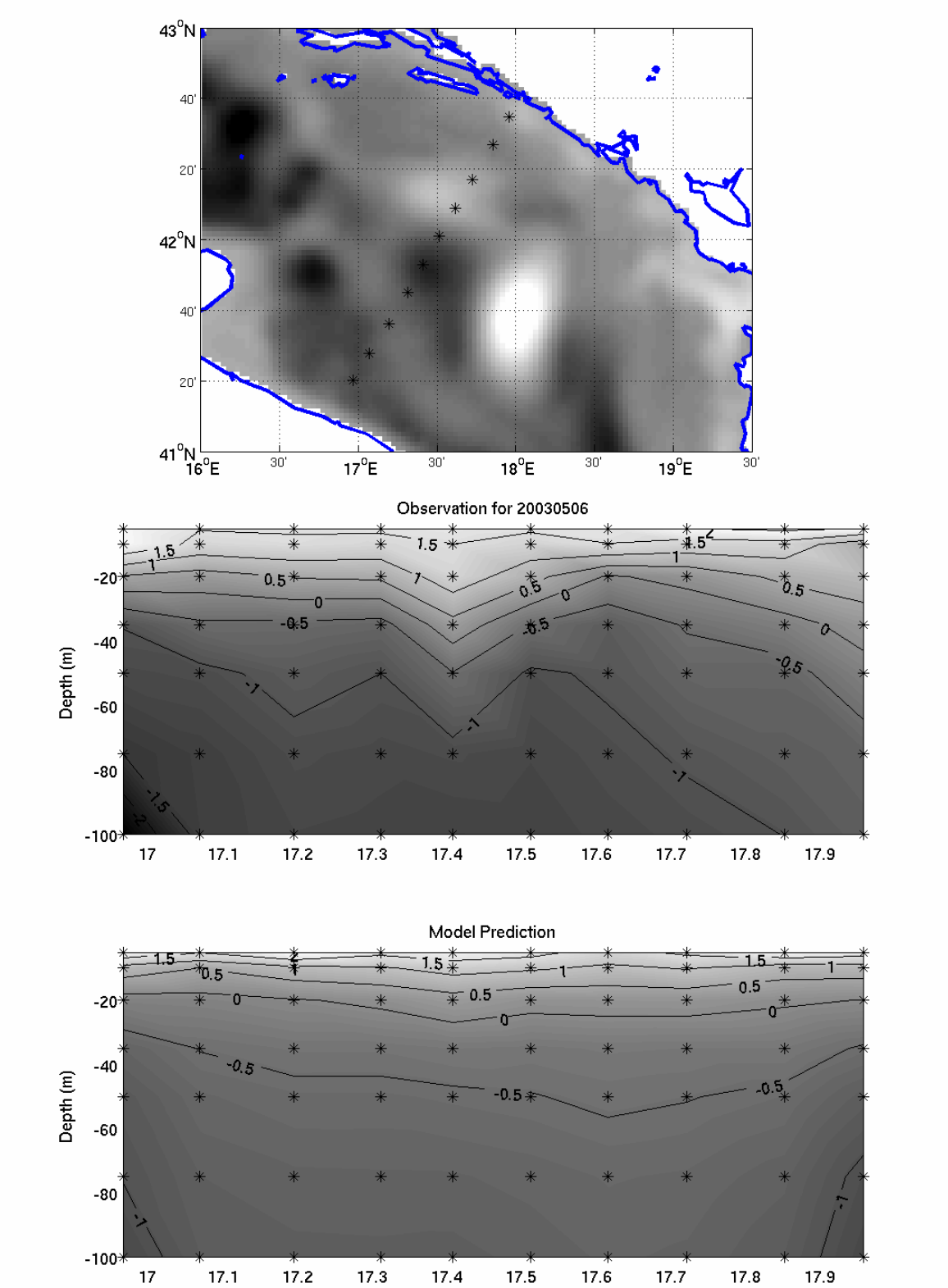

Fig.14 (Upper panel) Surface Elevation daily mean from model output for 2003-05-06**.** Also the XBT stations positions are shown. In the middle and bottom panels the vertical section of observed and simulated temperature anomaly along the XBT track are reported (°C).

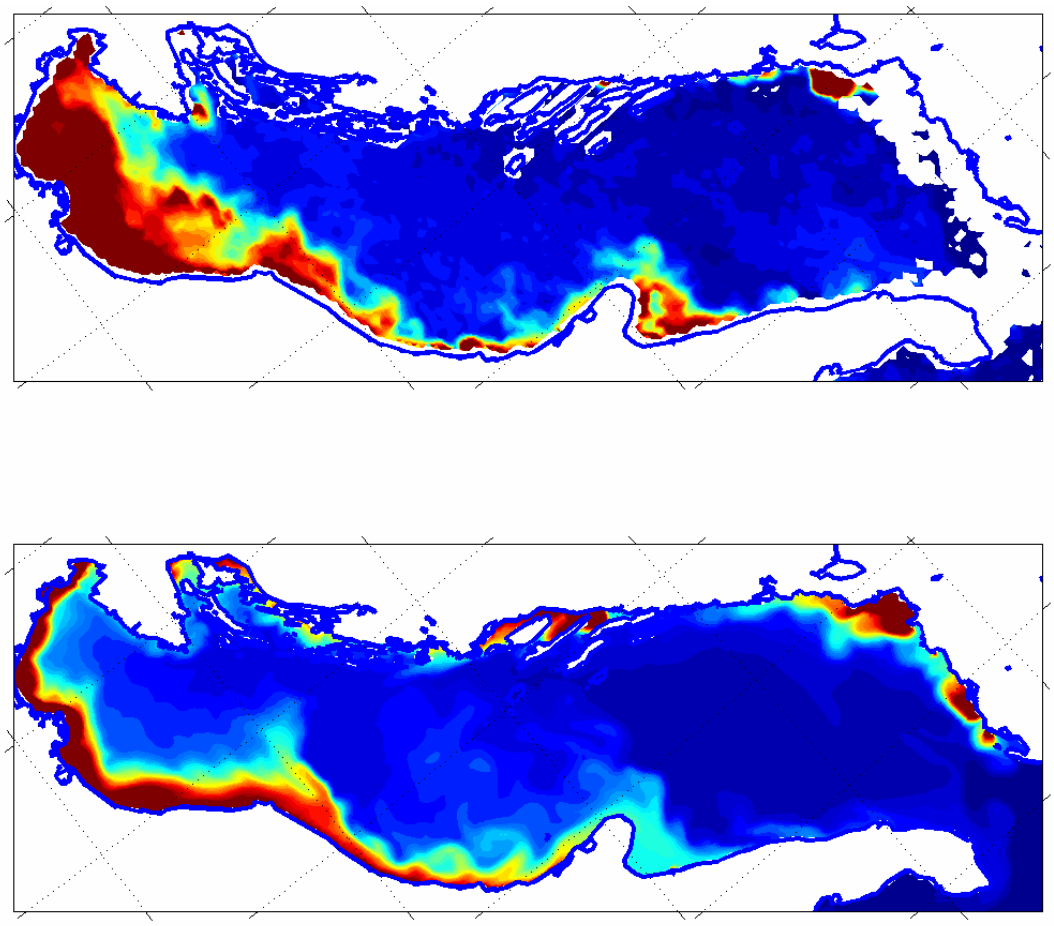

Fig.15 Comparison between Satellite Chlorophyll from SeaWIFS (Courtesy of Lia Santoleri, GOS-CNR, Rome, Italy) and model predicted sea surface salinity for May 4, 2003.